Responses of wind erosion to climate-induced vegetation changes on the Colorado Plateau

Seth M. Munson[a,1], Jayne Belnap[a], and Gregory S. Okin[b]

[a]US Geological Survey, Southwest Biological Science Center, Canyonlands Research Station, 2290 South West Resource Boulevard, Moab, UT 84532; and [b]Department of Geography, University of California, Los Angeles, CA 90095

Edited by William H. Schlesinger, Cary Institute of Ecosystem Studies, Millbrook, NY, and approved January 25, 2011 (received for review October 6, 2010)

Projected increases in aridity throughout the southwestern United States due to anthropogenic climate change will likely cause reductions in perennial vegetation cover, which leaves soil surfaces exposed to erosion. Accelerated rates of dust emission from wind erosion have large implications for ecosystems and human well-being, yet there is poor understanding of the sources and magnitude of dust emission in a hotter and drier climate. Here we use a two-stage approach to compare the susceptibility of grasslands and three different shrublands to wind erosion on the Colorado Plateau and demonstrate how climate can indirectly moderate the magnitude of aeolian sediment flux through different responses of dominant plants in these communities. First, using results from 20 y of vegetation monitoring, we found perennial grass cover in grasslands declined with increasing mean annual temperature in the previous year, whereas shrub cover in shrublands either showed no change or declined as temperature increased, depending on the species. Second, we used these vegetation monitoring results and measurements of soil stability as inputs into a field-validated wind erosion model and found that declines in perennial vegetation cover coupled with disturbance to biological soil crust resulted in an exponential increase in modeled aeolian sediment flux. Thus the effects of increased temperature on perennial plant cover and the correlation of declining plant cover with increased aeolian flux strongly suggest that sustained drought conditions across the southwest will accelerate the likelihood of dust production in the future on disturbed soil surfaces.

arid | horizontal flux | land use | national park | threshold shear velocity

Low perennial vegetation cover in arid regions of the southwestern United States leaves the soil surface exposed to wind erosion. Enhanced aridity due to anthropogenic climate change (1) is likely to result in declines of already low vegetation cover in the future, increasing the risk of wind erosion. Dust emission caused by wind erosion has received considerable attention because of its far-reaching effects on ecosystems, including the loss of nutrients and water-holding capacity from source areas (2), changes to climate and global energy balance in areas where dust is entrained in the atmosphere (3), fertilization of terrestrial and marine ecosystems (2, 4), in addition to decreases in snow albedo, causing earlier and faster snowmelt and river runoff in sink areas (5). Dust emission has also attracted interest due to its socioeconomic consequences, including property damage, declines in agricultural productivity, and health and safety hazards (6). Given the potentially large impact of dust emission, it is crucial to make predictions about the amounts and sources of dust emission under future climate change scenarios. Such predictions require an understanding of the temporal dynamics among climate, vegetation, and wind erosion across a spatially heterogeneous landscape.

The Colorado Plateau is an erosional landscape in the southwestern United States that is particularly susceptible to extreme fluctuations in climate because it is at the boundary of subtropical and midlatitude circulation regimes and influenced by El Niño-Southern Oscillation/Pacific Decadal Oscillation cycles (7). Low perennial vegetation cover (<40%) in grasslands and shrublands provides some protection from erosional forces in lower elevation regions, whereas biological soil crust (BSC; composed of cyanobacteria, mosses, and lichens) contributes to soil stability on unvegetated surfaces by binding soil particles together and creating surface roughness (8). Here we couple 20 y of vegetation monitoring across four well-protected national park areas of the Colorado Plateau (Fig. 1) with a wind erosion model to show how changes in climate can indirectly affect dust emission by influencing plant cover of dominant species and functional types. We compare the susceptibility of different plant communities to wind erosion and compare how perennial vegetation cover relative to BSC influences flux response with increasing soil disturbance.

Results and Discussion

During the 20-y study period, regional mean annual temperature in the national park areas increased significantly by 0.16 °C per year from 1989 to 1998 and declined by 0.04 °C from 1998 to 2008 (Fig. 2*A*). There was high interannual variability in precipitation, which ranged from 122 mm in 1989 to 309 mm in 2006 (Fig. 2*B*). Peak wind speeds in the region over this time period primarily occurred in the spring and reached 15.0–25.0 $m\,s^{-1}$ (Fig. 3). These are wind speeds that have generated high rates of sediment transport, as measured by dust traps and saltation sensors (9), as well as satellite imagery, which has detected expansive dust plumes over the western United States (http://sgst.wr.usgs.gov/dust_monitoring/dust-events).

We assessed plant cover in relationship to the past 20 y of climate variability by plant community type across the national park areas, which included perennial grasslands and three distinct shrubland communities characterized by the dominant species. The canopy covers of certain perennial plant species and functional types declined with increasing mean annual temperature in the previous year (12 mo preceding vegetation measurements; pMAT) and were less sensitive to monthly or annual precipitation. Although this result may be influenced by the high spatial variability of precipitation on the Colorado Plateau that can cause discrepancies between precipitation at the long-term weather station and vegetation plot, it provides a critical prediction for plant response to warmer future temperatures in the region. Because perennial plant species on the Colorado Plateau tolerate maximum temperatures higher than those recorded during this study (10, 11), the negative relationships with increasing temperature were likely caused by temperature-induced water stress resulting from high transpiration and evaporation from shallow soil depths. Although pMAT was the climatic factor that explained the most variation in perennial cover, there was a large amount of variance in cover through space and time that could be explained by soil and physical characteristics. We used vegetation

Author contributions: S.M.M. and J.B. designed research; S.M.M. and J.B. performed research; G.S.O. contributed new reagents/analytic tools; S.M.M. analyzed data; and S.M.M., J.B., and G.S.O. wrote the paper.

The authors declare no conflict of interest.

This article is a PNAS Direct Submission.

[1]To whom correspondence should be addressed. E-mail: smunson@usgs.gov.

This article contains supporting information online at www.pnas.org/lookup/suppl/doi:10.1073/pnas.1014947108/-/DCSupplemental.

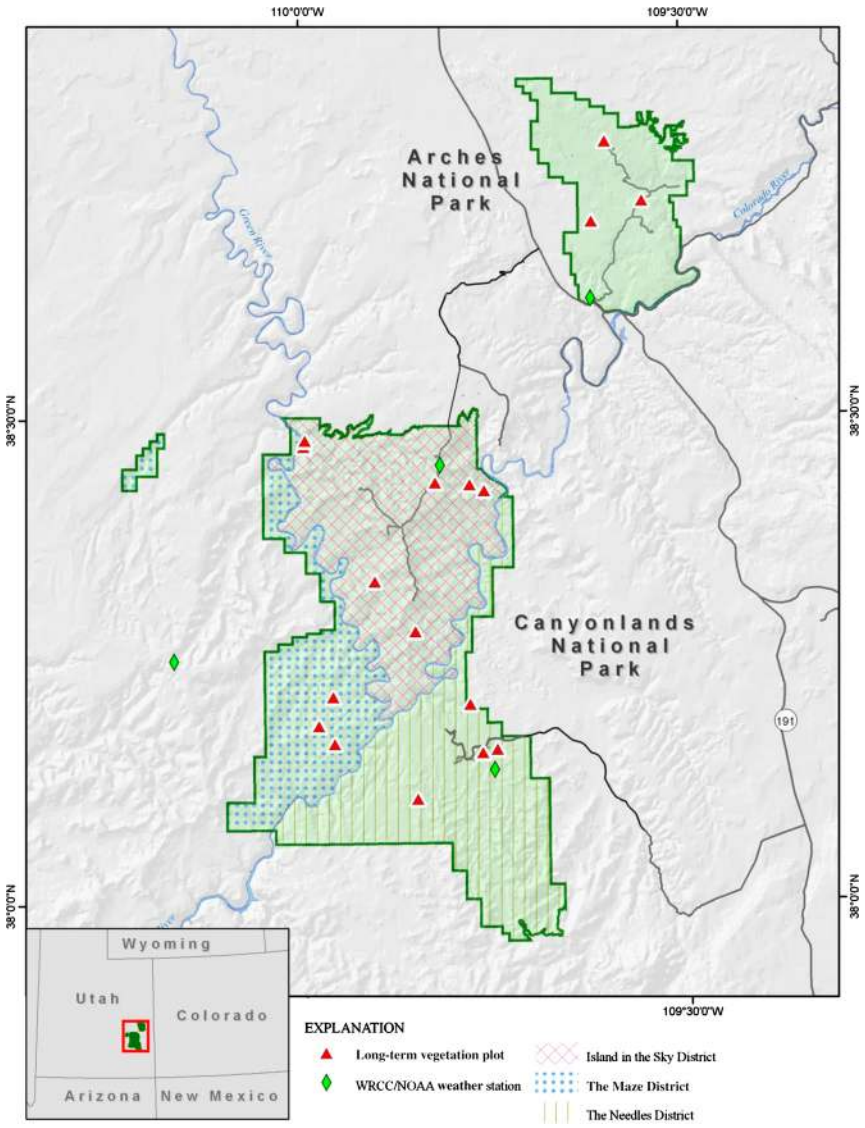

Fig. 1. Map of the long-term vegetation plots and Western Regional Climate Center (WRCC)/National Oceanic and Atmospheric Administration (NOAA) weather stations in the four national park areas on the Colorado Plateau in southeastern Utah.

monitoring results and soil stability measurements as inputs into a field-validated wind erosion model to compare the potential for wind erosion and dust emission among plant community types at peak wind speeds and determined how past climate variability has indirectly affected the potential for wind erosion and dust emission by its influence on perennial vegetation cover at a regional scale.

Perennial grasses declined by 8.0% canopy cover per 1 °C increase in pMAT, which contributed to a 6.6% decline of all perennial vegetation canopy cover across perennial grasslands (Fig. 4*A*). Perennial grasses were likely susceptible to temperature because they derive nearly 85% of their moisture from evaporation-prone shallow soil depths on the Colorado Plateau, compared to 54% for shrubs (12). Perennial grasslands had well-developed BSC, which did not significantly change with climatic variation during the study period. Although there is evidence that warmer and drier conditions in the future may lead to regional declines of lichens and mosses, cyanobacteria and other crust organisms are likely to be less sensitive and continue to provide soil surface stability (13). However, land use disturbance that occasionally occurs inside and frequently occurs outside the national park areas can break up BSC and greatly reduce the integrity of the soil surface (14).

Well-developed BSC in perennial grasslands was associated with high threshold shear velocity [the minimal shear velocity required to initiate wind erosion; (15)] and prevented aeolian sediment flux during simulated high-speed wind events. Aeolian sediment flux is primarily composed of saltating particles (horizontal flux), which are responsible for most soil deflation and downwind sediment deposition (16). These particles have high kinetic energy and accelerate erosion by bombarding the soil surface, releasing suspension-sized particles (<50 μm: vertical flux) that are otherwise strongly held to the surface by cohesive forces. This sandblasting causes a linear relationship between horizontal and vertical (dust) aeolian flux (17, 18), allowing us to use horizontal aeolian sediment flux as a proxy for dust emission rate.

When we simulated a high intensity soil disturbance by systematically reducing the threshold shear velocities (TSVs) of BSCs to values equivalent to driving over them twice with a vehicle (14), declines in canopy cover of perennial grasses resulted in an exponential increase in modeled aeolian sediment flux from 4 $g\,m^{-1}\,min^{-1}$ (at 10.0 °C pMAT) to 26 $g\,m^{-1}\,min^{-1}$ (at 13.5 °C pMAT) following a 15.0 $m\,s^{-1}$ wind event (Fig. 4*B*). These rates were within the range of values reported for similar wind conditions on a variety of uncrusted soil surfaces (17, 18) and intermediate in magnitude compared to shrubland communities. The flux rates reported from sediment trap samplers at sites with similar soils in perennial grassland and shrubland communities (19, 20) were considerably lower than our estimates. However, the samplers integrate flux over a much longer period of time, during high and low wind speed events, and our intention was

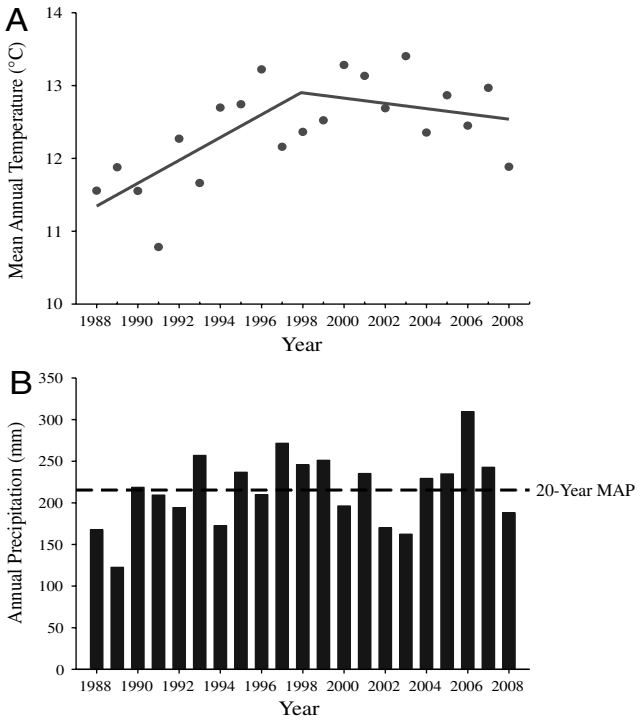

Fig. 2. Regional mean annual temperature (°C) from 1988 to 2008 for all WRCC/NOAA weather stations in the national park areas with fitted piecewise regression ($P < 0.0001$) (*A*). Annual precipitation (mm) from 1988 to 2008 for all WRCC/NOAA weather stations in the national park areas and 20-y mean annual precipitation (MAP) (*B*).

to characterize elevated rates of transport during high wind speed events. Increases in aeolian sediment flux with increasing temperature in perennial grasslands would have been higher if not for the expansion of shrub cover by species with rapid vegetative reproduction (e.g., *Ephedra* spp., *Ceratoides lanata*). This change in flux has relevance at a broad spatial scale due to the expansion of shrubs into grass-dominated plant communities throughout the Southwest (21, 22). Although shrubs generally have larger unvegetated gap sizes than grasses, their taller stature contributes to aerodynamic roughness and more effectively reduces shear stress on the downwind soil surface (23). Modeled aeolian sediment flux increased quadratically as wind speed increased, such that flux was 310 g m^{-1} min^{-1} (at 10.0 °C pMAT) to 780 g m^{-1} min^{-1} (at 13.5 °C pMAT) following a 25.0 m s^{-1} wind event (Fig. 4*B*).

Previous research has suggested that shrublands are more susceptible to wind erosion and dust emission than grasslands (19, 20, 24, 25). Our results suggest that there can be considerable variation in aeolian sediment flux in shrubland communities depending on the cover and height of the dominant shrub species. Because most shrubland communities also had high BSC, we simulated the same high intensity soil disturbance as perennial grasslands. Shrublands dominated by short-statured (approximately 50 cm average height) *Coleogyne ramosissima* had modeled aeolian sediment fluxes that were comparable to perennial grasslands (10 g m^{-1} min^{-1} with a wind speed of 15.0 m s^{-1}; 570 g m^{-1} min^{-1} with a wind speed of 25.0 m s^{-1} Fig. 4*D*), whereas shrublands codominated by the tall-growing (approximately 100 cm average height) *Artemisia tridentata* and *Sarcobatus vermiculatus* had very low modeled flux (0.2 g m^{-1} min^{-1} with a wind speed of 15.0 m s^{-1}; 150 g m^{-1} min^{-1} with a wind speed of 25.0 m s^{-1}; Fig. 4*F*), even when soils were disturbed. These results are consistent with field observations of generally low dust emission from these tall-statured shrub communities with or without soil disturbance (26). Modeled aeolian sediment flux in both *Coleogyne* and *Artemisia*/*Sarcobatus* shrubland types did not change with increases in pMAT because there were no significant changes in perennial canopy cover (Fig. 4 *C* and *E*). Therefore, these plant communities may be more resistant to wind erosion and dust emission with warmer and drier conditions in the future. However, most shrublands dominated by *Artemisia* and *Sarcobatus* in this study were near intermittently flowing streams where these shrubs were likely buffered from high temperatures because they had increased water availability. Where these communities occurred on a very high (>10 m) alluvial terrace, lack of access to this supplemental water likely caused declines in canopy cover of both of these shrubs as temperatures increased (Fig. 4*E*, *Inset*). This change in vegetation cover increased modeled aeolian sediment flux from 290 g m^{-1} (at 12.5 °C pMAT) to 740 g m^{-1} min^{-1}

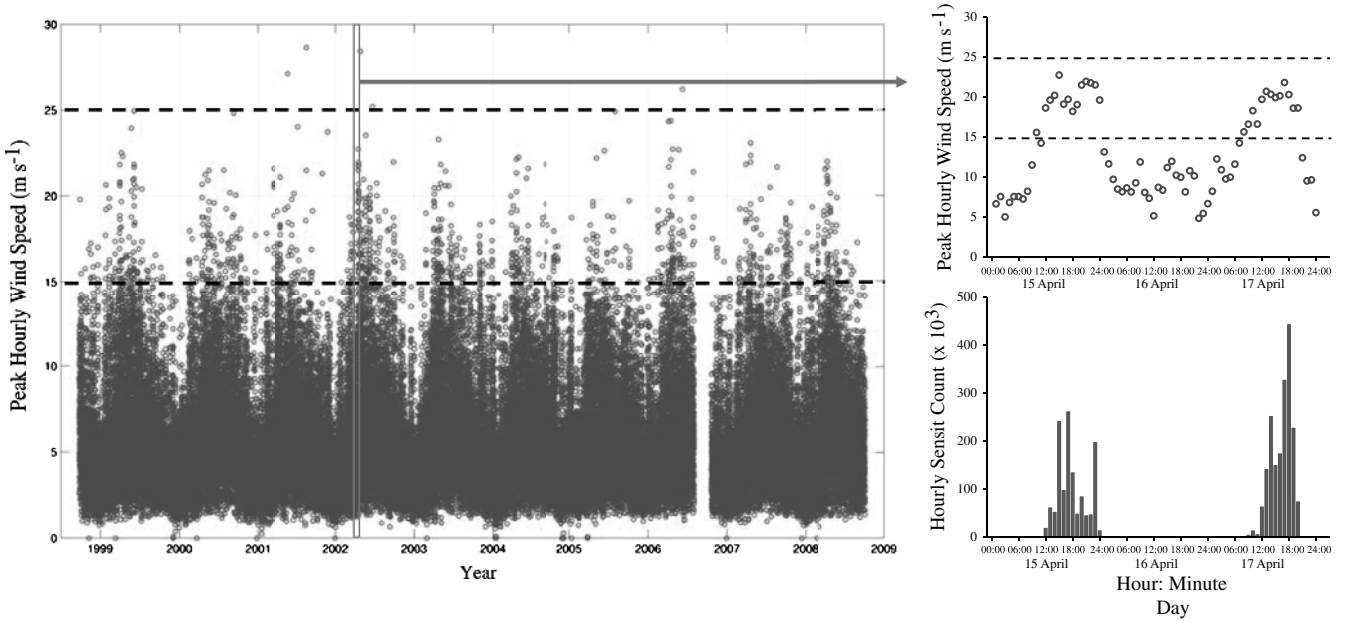

Fig. 3. One-hour peak wind speeds (m s^{-1}) at 3 m height at the Dugout Ranch near the study area from 1998 to 2008. Wind speeds of 15.0–25.0 m s^{-1} used in this study shown by dashed lines. Two day time period in mid-April 2002 highlighted by gray box and corresponding hourly Sensit counts, which are an index of sediment movement. Data obtained from http://gec.cr.usgs.gov/info/sw/clim-met.

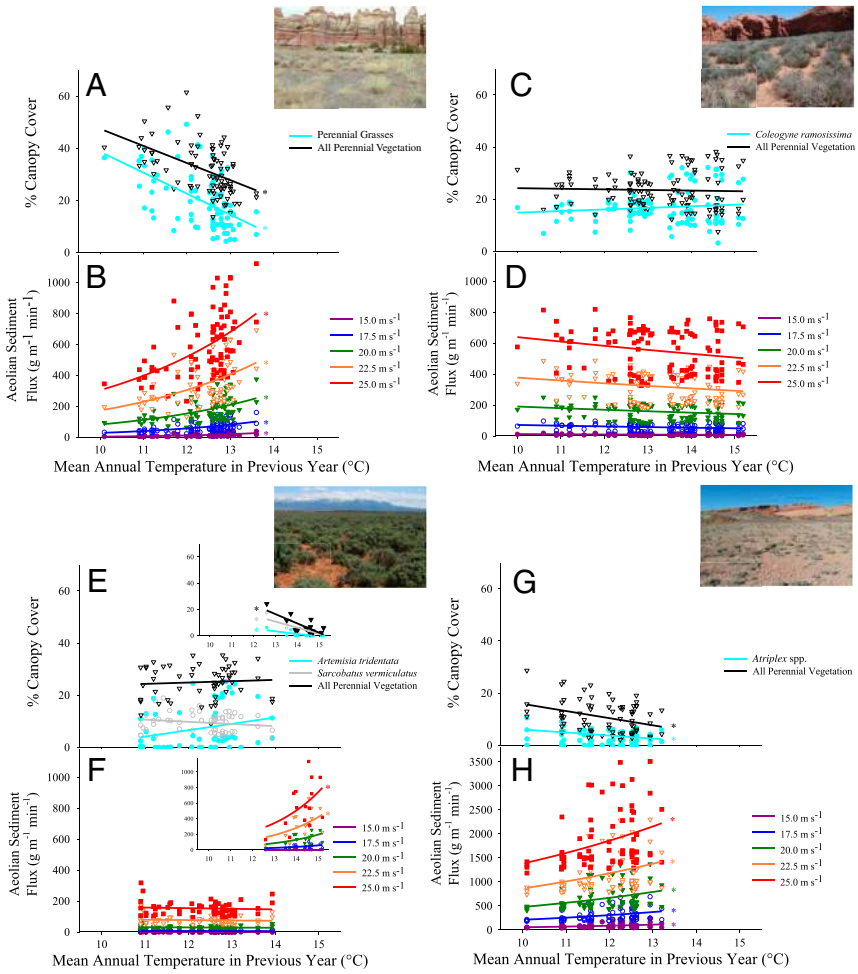

Fig. 4. Dominant plant species and functional type canopy cover (*A*, *C*, *E*, and *G*) and modeled aeolian sediment flux (*B*, *D*, *F*, and *H*) at five wind speeds (15.0, 17.5, 20.0, 22.5, and 25.0 m s^{-1}) in relationship to mean annual temperature in the previous year in perennial grasslands ($N = 6$; *A* and *B*), shrublands dominated by *Coleogyne ramosissima* ($N = 6$; *C* and *D*), *Artemisia tridentata* and *Sarcobatus vermiculatus* ($N = 4$; *E* and *F*), and dwarf *Atriplex* species ($N = 4$; *G* and *H*). Significant ($P < 0.05$) regressions shown by an asterisk (*) for (*A*) Perennial grasses: $y = -8.04x + 119.1$, $r^2 = 0.28$; all perennial vegetation: $y = -6.57x + 113.2$, $r^2 = 0.25$; aeolian sediment flux: $y = 0.02e^{0.54x}$, $r^2 = 0.26$ (15.0 m s^{-1}); $y = 0.77e^{0.36x}$, $r^2 = 0.22$ (17.5 m s^{-1}); $y = 3.65e^{0.31x}$, $r^2 = 0.23$ (20.0 m s^{-1}); $y = 9.96e^{0.29x}$, $r^2 = 0.24$ (22.5 m s^{-1}), $y = 20.7e^{0.27x}$, $r^2 = 0.25$ (25.0 m s^{-1}). (*C*, *Inset*) *Artemisia tridentata*: $y = -2.03x + 29.8$, $r^2 = 0.49$; *Sarcobatus vermiculatus*: $y = -4.60x + 70.5$, $r^2 = 0.51$, all perennial vegetation: $y = -7.09x + 108.7$, $r^2 = 0.57$; aeolian sediment flux: $y = 1.09e^{0.40x}$, $r^2 = 0.24$ (22.5 m s^{-1}), $y = 2.36e^{0.38x}$, $r^2 = 0.25$ (25.0 m s^{-1}). (*D*) *Atriplex* spp.: $y = -1.17x + 17.8$, $r^2 = 0.24$; all perennial vegetation: $y = -2.74x + 43.3$, $r^2 = 0.12$; aeolian sediment flux: $y = 5.35e^{0.23x}$, $r^2 = 0.11$ (15.0 m s^{-1}), $y = 31.8e^{0.19x}$, $r^2 = 0.12$ (17.5 m s^{-1}), $y = 88.7e^{0.17x}$, $r^2 = 0.12$ (20.0 m s^{-1}), $y = 181.3e^{0.16x}$, $r^2 = 0.12$ (22.5 m s^{-1}), $y = 313.8e^{0.15x}$, $r^2 = 0.12$ (25.0 m s^{-1}).

(at 15 °C pMAT) following a 25.0 m s^{-1} wind event (Fig. 4*F*, *Inset*). Limited access to groundwater or declining water tables may increase shrub mortality in this shrubland community (27) under future climate scenarios, creating conditions suitable for wind erosion and dust emission.

Shrublands dominated by dwarf *Atriplex* species (*A. confertifolia*, *A. gardnerii*, and *A. corrugata*) had relatively low perennial vegetation canopy cover (<20%) and height (approximately 30 cm) compared to other plant communities (Fig. 4*G*). Both *Atriplex* spp. and all perennial vegetation canopy cover decreased by 1.3% and 2.7%, respectively, per 1 °C increase in pMAT. *Atriplex* species likely declined because they have an extensive fine shallow root system (28) and occurred on shallow fine-textured clay soils, which are vulnerable to high evaporative losses. Low and decreasing shrub cover resulted in the highest modeled aeolian sediment flux of all plant communities following a high intensity soil disturbance. Modeled aeolian sediment flux increased exponentially with increases in pMAT from 56 g m^{-1} min^{-1} (at 10 °C pMAT) to 111 g m^{-1} min^{-1} (at 13 °C pMAT) following a 15.0 m s^{-1} wind event and from 1,400 to 2,160 g m^{-1} min^{-1} over the same temperature gradient following a 25.0 m s^{-1} wind event (Fig. 4*H*). Unlike other plant communities, BSC development in dwarf *Atriplex* plots ranged widely, as did the amount of perennial vegetation in the interspace of *Atriplex* shrubs, resulting in high variability in aeolian sediment flux among plots.

To examine the soil surface protection offered by BSC and its interaction with perennial vegetation cover, we determined how plots with low and high BSC in combination with low and high perennial vegetation cover influenced flux with increasing soil disturbance intensity in the dwarf *Atriplex* plant community. Plots in this plant community were within the same national park area (Island in the Sky) and experienced a similar gradient in temperature, thereby affecting perennial vegetation cover. Plots dominated by *Atriplex* spp. that had well-developed BSC (class >3; Murphy Hogback and Taylor Canyon 1) provided complete protection against wind erosion during a simulated wind event of 17.5 m s^{-1}, even with low perennial vegetation canopy cover following a low intensity [walking over crusts with lug-soled boots; (14)] soil disturbance (Fig. 5*A*). Biological soil crust on the same plots dampened flux to some degree following a medium intensity (driving once over crusts once with a vehicle) soil disturbance (Fig. 5*B*). This suggests that keeping soil structure intact, especially where crusts are present, may provide the greatest barrier against wind erosion and dust emission in arid regions (14, 29).

Additional protection from wind erosion was provided by perennial vegetation, until perennial canopy cover fell below 10%. Plots with cover above this threshold (Murphy Hogback and Amoeba Butte) were relatively well protected from wind erosion, whereas plots that had cover that fell below this threshold (Taylor Canyon 1 and 2), experienced substantial increases in modeled aeolian sediment flux (Fig. 5 *A*–*C*). Our results indicate that shrub cover falling below this threshold in dwarf *Atriplex* plant communities was related to increasing temperature (Fig. 4*G*). Other studies have also found that flux dramatically increased when vegetation canopy cover fell below 10–15% (30, 31), suggesting a possible wind erosion threshold for arid plant communities. Importantly, our results indicate that this threshold is mediated by plant height, as perennial vegetation canopy cover in tall-statured *Artemisia*/*Sarcobatus*-codominated shrublands fell

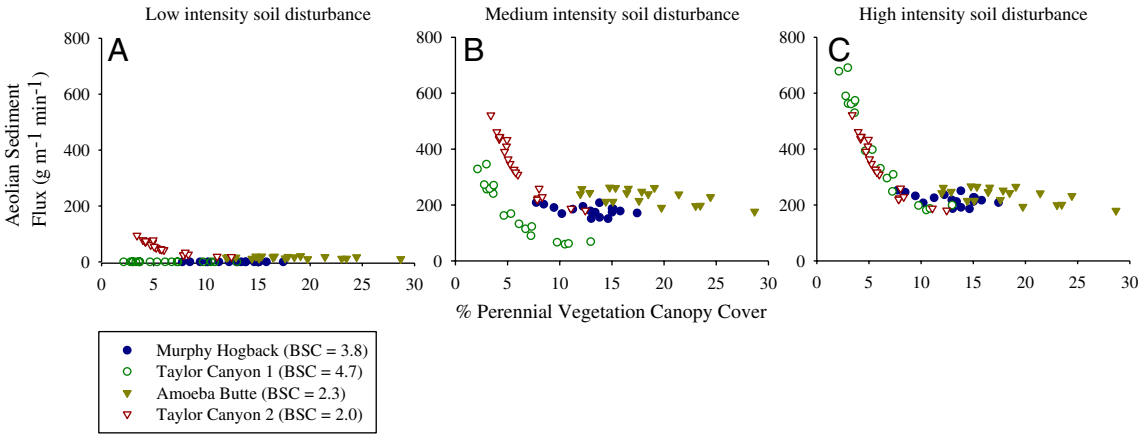

Fig. 5. Aeolian sediment flux following a 17.5 m s^{-1} wind event in relation to percent perennial vegetation canopy cover with low (*A*), medium (*B*), and high (*C*) intensity soil disturbances on four plots in dwarf *Atriplex* shrublands. Plots varied in perennial vegetation cover and average BSC development class (1, low; 6, high).

below 10%, but did not produce high flux. Because protection by BSC from wind erosion was eliminated following a high intensity soil disturbance, perennial vegetation cover became the only protection from wind erosion (Fig. 5*C*). Therefore, maintenance of vegetation cover above a minimum amount for a given plant community is extremely important in areas where there is little or no crust to protect soil surfaces.

Conclusions

Our results suggest that increased temperatures associated with climate change will indirectly lead to increased wind erosion and dust emission on the Colorado Plateau. Long-term monitoring of climate and vegetation in national parks demonstrates declines in the dominant perennial vegetation cover in grasslands and dwarf *Atriplex* shrublands with increases in temperature, which can lead to exponential increases in wind erosion. Dominant shrubs in *Coleogyne* and *Artemisia*/*Sarcobatus* shrubland communities may be better buffered against changes in perennial vegetation with increasing temperatures and therefore more resistant to dust emission during high wind speeds. The soil surface protection offered by perennial vegetation cover relative to BSC increased with soil disturbance, with important thresholds in flux occurring below 10% perennial vegetation canopy cover and BSC developmental class of 3, which is the class at which lichens and mosses provide additional protection (32). Well-developed BSCs prevented aeolian sediment flux during simulated high-speed wind events, which is consistent with observations in the field (14, 29). However, when such protection was reduced, the relative modeled aeolian sediment flux among Colorado Plateau plant communities on disturbed soils was lowest in *Artemisia*/*Sarcobatus* Shrublands < Perennial Grasslands = *Coleogyne* Shrublands < dwarf *Atriplex* Shrublands. Simulations of wind erosion were a useful tool to determine how perennial vegetation canopy cover and BSC influenced aeolian sediment flux in response to climate change. Future improvements to wind erosion modeling coupled with experimental and observational data can only serve to build on this important first step to understanding how climate change affects wind erosion in arid regions.

Methods

The study area comprises four national park areas in southeastern Utah [Arches—310 km^2, and the three districts of Canyonlands National Park —1,366 km^2 (the Needles, Island in the Sky, and the Maze)] lying between 37.96°–38.85°N and 109.47°–110.24°W and ranging in elevation from 1,100 to 2,100 m (Fig. 1). These park areas are relatively well protected from human land use disturbance, but were grazed by livestock before the mid-1960s–1970s. Permanent vegetation plots were established across the major plant communities in the four national park areas in 1989 to monitor changes in plant species canopy cover. A minimum of three replicate plots (spaced 1–70 km apart) were used for each major plant community found in the parks. At each plot, 100 (0.5 m × 0.5 m) permanently marked quadrats were evenly spaced 2 m apart along 100-m transects. Canopy cover for each species was annually recorded in the quadrats in April or early May. A visual assessment of soil surface stability in each quadrat was made by determining the developmental stage [(*i*) least developed—(*vi*) most developed)] of BSC (32). We obtained total monthly precipitation and mean monthly temperature for each plot from the nearest weather station in the Western Regional Climate Center network (http://www.wrcc.dri.edu) and 1-h peak wind speeds from a CLIM-MET (climate impact meteorological) station at the Dugout Ranch near the long-term vegetation plots (http://gec.cr.usgs.gov/info/sw/clim-met).

We assessed plant relationships to past climate variability by plant community type, which included perennial grasslands and three distinct shrubland communities characterized by the dominant species [(*i*) *Coleogyne ramosissima*, (*ii*) *Artemisia tridentata*/*Sarcobatus vermiculatus*, and (*iii*) *Atriplex* species—*A. confertifolia, A. gardneri, and A. corrugata*]. We used only plots that were measured in all or most years of the study in the analysis. Average canopy cover of dominant plant species and functional types (species with the same life form, lifespan, and structure) within a plant community was regressed against total monthly and annual precipitation and mean monthly and annual temperature across all years with lag times up to 2 y (33). We used an arcsine square root transformation on cover when assumptions of normality and homogeneity of variance were not met and present the back-transformed values.

We simulated wind erosion on the same plots that were monitored for 20 y using a shear-stress partitioning model, which provides a way to scale from flux at a single point using characteristics of the soil surface to the landscape scale flux by explicitly considering the spatial distribution of vegetation on the soil surface (34). The wind erosion model accounts for the depression of surface shear velocity in the wake of plants and uses the size distribution of erodible gaps between plants to account for spatial variability of shear stress experienced by the soil. The model is formulated probabilistically, using the probability distribution function of the nearest upwind plant. Total horizontal aeolian sediment flux, Q_{Tot} (expressed in units of mass per unit distance perpendicular to the wind per unit time) is calculated as the sum of different sources weighted by the fraction of the area that they occupy:

$$Q_{\mathrm{Tot}} = \int_0^{\infty} P_d\left(\frac{x}{h}\right) q_{\frac{x}{h}} d\left(\frac{x}{h}\right), \qquad [1]$$

where $P_d(\frac{x}{h})$ is the probability that any point in the landscape is x distance from the nearest upwind plant expressed in units of height (h) of that plant, and $q_{\frac{x}{h}}$ is the horizontal aeolian sediment flux for a point $\frac{x}{h}$ away from the nearest upwind plant. At small distances from a plant, $q_{\frac{x}{h}}$ is significantly less than flux in the absence of vegetation. We report horizontal aeolian sediment flux because vertical dust flux, F_{Tot}, is a proportion of horizontal aeolian sediment flux [$F_{\mathrm{Tot}}/Q_{\mathrm{Tot}} = 1 \times 10^{-3} - 1 \times 10^{-4}$ m^{-1} on similar soils; (17)], and horizontal aeolian sediment flux contains larger soil particles necessary to maintain dust emission from the soil surface. $P_d(x)$ of vegetation in arid regions can be represented by the exponential equation (35)

$$P_d(x) = \frac{e^{\frac{-x}{\bar{L}}}}{\bar{L}}, \qquad [2]$$

where $\bar{L}$ is the average gap size between plants. $\bar{L}$ was determined from an empirical relationship between perennial vegetation canopy cover and average gap size in perennial grasslands ($r^2 = 0.92$, $P < 0.0001$) and shrublands ($r^2 = 0.97$, $P < 0.0001$) on plots used for this study and adjacent areas (Fig. S1). Because canopy cover of annual species is highly variable and provides low erosion resistance in a drought year, we included only perennial vegetation in the wind erosion simulations. Plant height (h) was determined by using the average height of each plant functional type weighted by its canopy cover in the plot. Aeolian sediment flux for a point $\frac{x}{h}$ distance from the nearest upwind plant is calculated using the formulation (36)

$$q_{\frac{x}{h}} = A\frac{\rho}{g}u_{*s}(u_{*s}^2 - u_{*t}^2), \quad [3]$$

where A is a dimensionless constant, ρ is the density of air, g is the acceleration of gravity, u_{*s} is the shear velocity, and u_{*t} is the TSV of the unvegetated soil surface. TSV is the shear velocity at which soil erosion begins (15). Okin explains more details of the model and parameterizes the model using experimental data (34). We derived TSV for each plot from an empirical relationship between the developmental stage of BSC and TSV ($r^2 = 0.57$, $P < 0.0001$; Fig. S2). Although BSC has a large influence on TSV in our study area, future improvements to estimating soil stability could include soil texture, chemistry, physical crusts, and gravel (17). We simulated decreases in soil stability by systematically lowering TSV according to relationships between TSV and disturbed, as well as undisturbed, BSC derived from wind tunnel experiments in the region (14). Disturbance consisted of three levels of intensity: walking over crusts with lug-soled boots (low intensity) and driving once (medium intensity) or twice (high intensity) over crusts with a vehicle.

To validate the wind erosion model for our study area, we fit TSVs experimentally derived from a wind tunnel on different soil types found in the national parks to the model and compared modeled flux to the rates of sediment yield generated in the wind tunnel. There was good agreement between modeled aeolian sediment flux and experimental aeolian sediment flux from the wind tunnel on different soil types in the study area (Fig. S3), with the slope (0.95) of the relationship not significantly different from 1 ($F = 0.06$, $P = 0.81$) and the intercept (1.5) not significantly different from 0 ($F = 0.00$, $P = 0.96$). Although a limitation to this validation is the use of point- instead of landcape-scale field estimates, the model has been shown to perform well across at intermediate spatial scales because it integrates the influence of soil stability with the spatial distribution of vegetation over a larger area.

We simulated five wind events of 15.0, 17.5, 20.0, 22.5, and 25.0 m s^{-1} at 3 m above the surface on each plot in every year vegetation and soil stability were measured. Although sediment transport can occur at much lower wind speeds, our intention was to characterize elevated rates of transport that occur in the study area. Because we expected aeolian sediment flux rates generated from wind erosion simulations to closely track changes in vegetation, flux rates were regressed against the same climatic variables that were significantly correlated to dominant plant species and functional type canopy cover.

ACKNOWLEDGMENTS. Thanks to M. E. Miller, T. Belote, and F. Urban for supplemental field data and helpful suggestions, M. McKee and A. Wight for compiling park datasets, as well as J. Li, C. Lawrence, and C. Vojta for reviews of earlier versions of this paper. Any use of trade, product, or firm names in this paper is for descriptive purposes only and does not imply endorsement by the US Government. A grant from the US Geological Survey Global Change Research Program supported this work.

1. Seager R, et al. (2007) Model projections of an imminent transition to a more arid climate in Southwestern North America. *Science* 316:1181–1184.
2. Reynolds R, Belnap J, Reheis M, Lamothe P, Luiszer F (2001) Aeolian dust in Colorado Plateau soils: Nutrient inputs and recent change in source. *Proc Natl Acad Sci* 98:7123–7127.
3. Sokolik I, Toon OB (1999) Incorporation of mineralogical composition into models of the radiative properties of mineral aerosol from UV to IR wavelengths. *J Geo Res* 104:9423–9444.
4. Piketh SJ, Tyson PD, Steffen W (2000) Aeolian transport from southern Africa and iron fertilization of marine biota in the south Indian Ocean. *S Afr J Sci* 96:244–246.
5. Painter TH, et al. (2010) Response of Colorado River runoff to dust radiative forcing in snow. *Proc Natl Acad Sci USA* 107:17125–17130.
6. Griffin DW, Kellogg CA, Shinn EA (2001) Dust in the wind: Long range transport of dust in the atmosphere and its implications for global public and ecosystem health. *Glob Change Hum Health* 2:20–33.
7. Schwinning S, Belnap J, Bowling DR, Ehleringer JR (2008) Sensitivity of the Colorado Plateau to change: Climate, ecosystems, and society. *Ecol Soc* 13:28.
8. Belnap J, Gardner JS (1993) Soil microstructure in soils of the Colorado Plateau: The role of the cyanobacterium *Microcoleus vaginatus*. *Great Basin Nat* 53:40–47.
9. Belnap J, et al. (2009) Sediment losses and gains across a gradient of livestock grazing and plant invasion in a cool, semi-arid grassland, Colorado Plateau, USA. *Aeolian Res* 1:27–43.
10. Loik ME, Harte J (1996) High-temperature tolerance of *Artemisia tridentata* and *Potentilla gracilis* under a climate change manipulation. *Oecologia* 108:224–231.
11. Hacke UG, Sperry JS, Pittermann J (2000) Drought experience and cavitation resistance in six shrubs from the Great Basin, Utah. *Basic Appl Ecol* 1:31–41.
12. Ehleringer JR (2001) Productivity of deserts. *Primary Productivity in Terrestrial Ecosystems*, eds HA Mooney and J Roy (Academic, San Diego), pp 345–362.
13. Belnap J, Phillips SL, Troxler T (2006) Soil lichen and moss cover and species richness can be highly dynamic: The effects of invasion by the annual exotic grass *Bromus tectorum* and the effects of climate on biological soil crusts. *Appl Soil Ecol* 32:63–76.
14. Belnap J, Gillette DA (1997) Disturbance of biological soil crusts: Impacts on potential wind erodibility of sandy desert soils in southeastern Utah. *Land Degrad Dev* 8:355–362.
15. Gilette DA, Adams J, Endo A, Smith D, Kihl R (1980) Threshold velocities for input of soil particles into the air by desert soils. *J Geophys Res* 85:5621–5630.
16. Gibbens RP, Tromble JM, Hennessy JT, Cardenas M (1983) Soil movement in mesquite dunelands and former grasslands of southern New Mexico from 1933 to 1980. *J Range Manage* 36:145–148.
17. Gillette DA (1978) A wind tunnel simulation of the erosion of soil: Effect of soil texture, sandblasting, wind speed, and soil consolidation on dust production. *Atmos Environ* 12:1735–1743.
18. Gillette DA, et al. (1997) Relation of vertical flux of particles smaller than 10 μm to total aeolian horizontal mass flux at Owens Lake. *J Geophys Res* 102:26009–26015.
19. Gillette DA, Pitchford AM (2004) Sand flux in the northern Chihuahuan desert, New Mexico, USA, and the influence of mesquite-dominated landscapes. *J Geophys Res* 109:F04003.
20. Bergametti G, Gillette DA (2010) Aeolian sediment fluxes measured over various plant/soil complexes in the Chihuahuan desert. *J Geophys Res* 115:F03044.
21. Schlesinger WH, et al. (1990) Biological feedbacks in global desertification. *Science* 247:1043–1048.
22. Archer SR, Schimel DS, Holland EA (1995) Mechanisms of shrubland expansion: Land use, climate or CO_2. *Climatic Change* 29:91–99.
23. Gillies JA, Nickling WG, King J (2002) Drag coefficient and plant form response to wind speed in three plant species: Burning Bush (*Euonymus alatus*), Colorado Blue Spruce (*Picea pungens* glauca), and Fountain Grass (*Pennisetum setaceum*). *J Geophys Res* 107:4760.
24. Grover HD, Musick HB (1990) Shrubland encroachment in southern New Mexico, U.S.A.: An analysis of desertification processes in the American Southwest. *Climatic Change* 17:305–330.
25. Breshears DD, Whicker JJ, Johansen MP, Pinder JE, III (2003) Wind and water erosion and transport in semiarid shrubland, grassland, and forest ecosystems: Quantifying dominance of horizontal wind-driven transport. *Earth Surf Proc Land* 28:1189–1209.
26. Sankey JB, Germino MJ, Glenn NF (2009) Aeolian sediment transport following wildfire in sagebrush steppe. *J Arid Environ* 73:912–919.
27. Naumburg E, Mata-Gonzalez R, Hunter RG, McLendon T, Martin DW (2005) Phreatophytic vegetation and groundwater fluctuations: A review of current research and application of ecosystem response modeling with an emphasis on Great Basin vegetation. *Environ Manage* 35:726–740.
28. Dobrowolski JP, Caldwell MM, Richards JH (1990) *Plant Biology of the Basin and Range, Ecological Studies*, eds CB Osmond et al. (Springer, Berlin), Vol 80, pp 243–292.
29. Belnap J (2003) *Biological Soil Crusts: Structure, Function, and Management, Ecological Studies*, eds J Belnap and OL Lange (Springer, Berlin), Vol 150, pp 339–347.
30. Lancaster N, Baas A (1998) Influence of vegetation cover on sand transport by wind: Field studies at Owens Lake, California. *Earth Surf Proc Land* 23:69–82.
31. Wiggs GFS, Thomas DSG, Bullard JE, Livingstone I (1995) Dune mobility and vegetation cover in the southwest Kalahari Desert. *Earth Surf Proc Land* 20:515–529.
32. Belnap J, Phillips SL, Witwicki DL, Miller ME (2008) Visually assessing the level of development and soil surface stability of cyanobacterially dominated biological soil crusts. *J Arid Environ* 72:1257–1264.
33. R Development Core Team (2008) R: A language and environment for statistical computing. (R Foundation for Statistical Computing, Vienna, Austria), http://www.r-project.org.
34. Okin GS (2008) A new model of wind erosion in the presence of vegetation. *J Geophys Res* 113:F02S10.
35. McGlynn IO, Okin GS (2006) Characterization of shrub distribution using high spatial resolution remote sensing: Ecosystem implication for a former Chihuahuan Desert grassland. *Remote Sens Environ* 101:554–566.
36. Shao Y, Raupauch MR, Findlater PA (1993) Effect of saltation bombardment on the entrainment of dust by wind. *J Geophys Res* 98:12719–12726.